Research Article

Wave loads by an oscillating water column in presence of bottom-mounted obstacle in the channel of finite width

P. Borah[1] · M. Hassan[1]

Abstract
In the present study, we solved the problem of diffraction in water waves with consists of a pair of vertical cylinders in a channel having finite width. It consists of a partially submerged floating hollow cylinder place above a fixed coaxial bottom-mounted obstacle. With the help of matched eigenfunction expansion, channel multipole and variables separation methods, the analytical expression of potentials are obtained. Using these analytical expressions of diffracted velocity potentials, we can derive the expressions of exciting forces exerted by the cylinders. The influence of various parameters viz draft of the hollow cylinder, radius of the cylinders, the gap between the cylinders and the width of the channel walls on the exciting forces have been investigated. The results have been validated by comparing our results with available results. All the observations are validated through suitable graphs.

Keywords Diffraction · Channel multipoles · Exciting force · Virtual boundary · Wavenumber

Mathematics Subject Classification 76B07 · 76B15

1 Introduction

Numerous hypothetical investigations have been performed to dissect the diffraction and radiation of water waves on a structure. Bharatkumar et al. [1] computed the first order forces and pressure on a pair of circular cylinders in a channel by using the Green's function method and the method of images. Bhatta and Rahman [2] solved the problem of diffraction and radiation to the water waves by a circular cylinder in uniform water depth. Bhattacharjee and Soares [4] calculated wave induced force acting on a floating rectangular structure placed in front a vertical wall in water of step type bottom. Buffer and Thomas [3] used multipole method to compute reflection and transmission coefficients for an array of cylinders in a channel. Hassan and Bora [5, 6] analyzed the diffraction problem by a couple of vertical cylinders. They evaluated the forces acting on the cylinders for various draft and radii of the cylinders. Kashiwagi [7] used three dimensional Green's function method to solve the problem of water waves by offshore structure in a channel. Kashiwagi [7] has also processed mean second-order drift forces on four truncated cylinders orchestrated in a square and contrasted his outcomes and exploratory information. Linton [8], Linton and Evans [9] and McIver and Bennett [12] applied multipole expansions method to solve the diffraction along with radiation problems of water wave by a cylinder in a channel. Martins-rivas and Mei [10] given linearized theory of an oscillating water column (OWC) on a straight coast. They evaluated the coefficients of apparent mass and radiation damping, and the chamber pressure. Martins-rivas and Mei [11] given the theoretically investigation of a single oscillating water column (OWC) situated at the tip of a long and thin breakwater. Neelamani et al. [14] approach the same problem who compared the experimental results with the theoretical results for a specific case of two circular cylinder.

✉ M. Hassan, mdhassan000@gmail.com; P. Borah, pankajborahmajuli@gmail.com | [1]Department of Mathematics, North Eastern Regional Institute of Science and Technology, Itanagar, Arunachal Pradesh 791 109, India.

SN Applied Sciences (2019) 1:1289 | https://doi.org/10.1007/s42452-019-1265-y

Received: 31 May 2019 / Accepted: 11 September 2019 / Published online: 26 September 2019

Thomas [15] utilized the image method to solve scattering and radiation problems for a single vertical circular cylinder in a channel. Thorne [16] derived multipoles in two and three dimensions which allow the clear arrangement of numerous issues. MacCamy and Fuchs [13] solved the diffraction problem by a vertical cylinder of discretionary water depth and derived analytical solution of diffracted potential. This solution is as yet utilized as a building configuration code. Wu et al. [17, 18] discussed the hydrodynamic coefficients and wave exciting force on a float over an arched body whose radius was smaller or larger than that of the float. Yeung and Sphaier [19] used the image method to solve scattering and radiation problems for a vertical circular cylinder in a channel, at times stretching out all through the whole water profundity. Zhu and Mitchell [20] solved the problem of diffraction of ocean wave by a hollow cylinder in an ocean of uniform depth and they used Galkerin's method to find the analytical solution of this problem. Zheng et al. [21] investigated the fulfilment of an oscillating water column(OWC) over a vertical structure in uniform water depth. the have valodated their results and then model is used to study the effect of the thickness of the chamber wall and the radius.

The study of the diffraction problem by a fixed structure can provide fundamental information about wave force on the structure. Our present investigation is also dealing with the diffraction problem by cylinderical stuctures which are placed on the centreline between the channel walls. It is thus important to understand the elucidation of the results of the wave tank testing of the offshore structures. Also it is necessary to evaluate how the tank walls impacts on quantities such as hydrodynamic forces on a fixed structure. In this paper, we consider two coaxial cylindrical structures in a channel of finite width, the upper one is partially submerged floating hollow cylinder which can be considered as oscillating water column (OWC) and the lower one is solid bottom-mounted obstacle which can be assumed solid cylindrical structure. The method to solve this problem is based on the construction of suitable multipoles for the channel problem which was developed by Linton and Evans [9]. Thus, when we consider a channel of water of uniform depth H and width $2d$ of channel walls, then suitable multipoles satisfy the Laplace's equation in our identified fluid region.

2 Mathematical model

We consider a pair of coaxial cylinders placed in an infinitely long channel of finite width $2d$ and depth of water is H. The pair of cylinders consists of one hollow cylinder which is partially merged in water and one solid cylinder which is bottom mounted. We also consider the radius of hollow cylinder is r_1 and the radius of bottom-mounted solid cylinder is r_2 ($r_1 \le r_2 < d$). Cartesian axes (x, y, z) are considered with x-axis taken parallel to the channel walls and $z-$ axis taken vertically upward. The origin is chosen at O which lies on the centreline of the channel walls in the mean of the undisturbed free surface of water as shown in Fig. 1. The polar coordinates r and θ are defined by

$$x = r\cos\theta \text{ and } y = r\sin\theta. \tag{1}$$

The regions are occupied by the hollow cylinder is given by $r < r_1$, $0 \le \theta < 2\pi$, $-e_1 \le z \le 0$ and occupied by the bottom-mounted cylinder is given by $r < r_2$, $0 \le \theta < 2\pi$, $-H \le z \le -h_2$.

By considering the linear water wave theory, the time harmonic velocity potential $\Phi(x, y, z, t)$ can be written as

$$\Phi(x,y,z,t) = Re[\phi(x,y,z)e^{-i\omega t}], \tag{2}$$

where i is an imaginary unit which is defined by its property $i = \sqrt{-1}$, t represents the time, ω is the angular frequency whereas Re represents the real part of the complex quantity in bracket and $\phi(x,y,z)$ be the spatial portion of the total potential satisfied to the following Laplace equation:

$$\frac{\partial^2\phi}{\partial x^2} + \frac{\partial^2\phi}{\partial y^2} + \frac{\partial^2\phi}{\partial z^2} = 0. \tag{3}$$

Then the total velocity potential can be written as

$$\phi = \phi_{inc} + \phi_d, \tag{4}$$

where ϕ_{inc} and ϕ_d are velocity potential due to incident wave and diffracted wave with the cylindrical structure, respectively. We divide the whole fluid region into three physical regions, namely I, II and III as indicated in Fig. 1. Let the velocity potentials in regions I, II and III are ϕ_d^I, ϕ_d^{II} and ϕ_d^{III}, respectively.

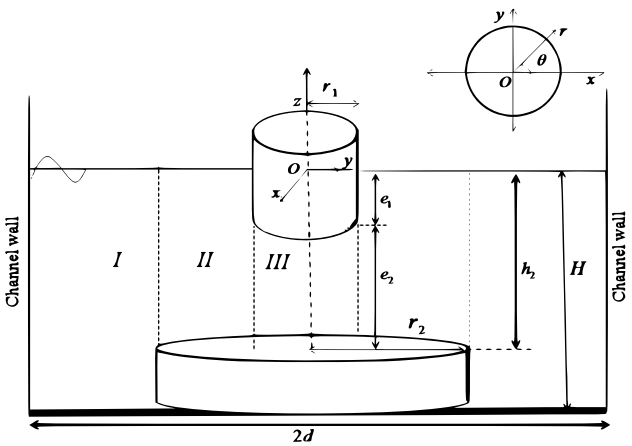

Fig. 1 Schematic of the device

Using separation of variable method, we obtain the vertical eigenfunctions for each region as shown in Fig. 1 and can be expressed as follows

$$f_m(z) = M_m^{-1/2}\cos[\lambda_m(z+H)], \text{ for the region } I, \tag{5}$$

$$g_m(z) = N_m^{1/2}\cos[\alpha_m(z+h_2)], \text{ for the region } II \text{ and } III, \tag{6}$$

where $M_m = \frac{1}{2}\left(1+\frac{\sin 2\lambda_m H}{2\lambda_m H}\right)$ and $N_m = \frac{1}{2}\left(1+\frac{\sin 2\alpha_m h_2}{2\alpha_m h_2}\right)$ and the eigenvalues λ_m and α_m can be determined from the following dispersion relations

$$\begin{cases} \lambda_0 = -ik, \quad \omega^2 = gk\tanh(kH), & m = 0 \\ \omega^2 = -g\lambda_m\tan(\lambda_m H), & m = 1,2,3,\ldots, \end{cases} \tag{7}$$

$$\begin{cases} \alpha_0 = -ik', \quad \omega^2 = gk'\tanh(kh_2), & m = 0 \\ \omega^2 = -g\alpha_m\tan(\alpha_m h_2), & m = 1,2,3,\ldots, \end{cases} \tag{8}$$

with k is the wave numbers in region I, k' is the wave number in II and III regions and the gravitational acceleration is g. Therefore the potential ϕ describing the diffraction wave field which satisfy the following Helmholtz equation

$$\frac{\partial^2\phi}{\partial x^2} + \frac{\partial^2\phi}{\partial y^2} - \lambda_m^2\phi = 0 \tag{9}$$

in the fluid region I as shown in Fig. 1.

The analytical expression of potential due to incident wave with unit amplitude from [13]

$$\phi_{inc} = -\frac{ig\cosh k(z+H)}{\omega\cosh(kH)}\sum_{m=0}^{\infty}\mu_m J_m(kr)\cos m\theta, \tag{10}$$

where Bessel function of the first kind is $J_m(.)$, and μ_m is written by

$$\mu_m = \begin{cases} 1, & m = 0 \\ 2i^m, & m > 0 \end{cases} \tag{11}$$

3 The governing equation of the problem

The diffracted velocity potential $\phi_d(x,y,z)$ fulfills the following governing equation and the boundary conditions

$$\nabla^2\phi_d = 0, \quad (-H < z < 0, -\infty < x < \infty, -d < y < d), \tag{12}$$

$$\frac{\partial\phi_d}{\partial z} - \frac{\omega^2}{g}\phi_d = 0; \quad (z = 0), \tag{13}$$

$$\frac{\partial\phi_d}{\partial z} = 0; \quad (z = -H, r \geq r_2; z = -h_2, r \leq r_2), \tag{14}$$

$$\frac{\partial(\phi_d+\phi_{inc})}{\partial r} = 0; \quad (-e_1 < z < 0,\ r = r_1;\ -H < z < -h_2,\ r = r_2), \tag{15}$$

$$\frac{\partial\phi_d}{\partial y} = 0; \quad (y = \pm d), \tag{16}$$

$$\lim_{r\to\infty}\sqrt{r}\left(\frac{\partial\phi_d}{\partial r} - ik\phi_d\right) = 0. \tag{17}$$

3.1 Matching conditions

To proceed in order to determine the unknown coefficients of the expression of velocity potentials, we introduce the proper matching conditions to preserve continuity fluid motion along the seeming interface and cylinder's boundaries as indicated in Fig. 1. Therefore, at $r = r_2$, we have

$$\phi_d^I = \phi_d^{II} \quad (-h_2 \leq z \leq 0), \tag{18}$$

$$\frac{\partial\phi_d^I}{\partial r} = \begin{cases} -\frac{\partial\phi_{inc}}{\partial r} & (-H \leq z \leq -h_2), \\ \frac{\partial\phi_d^{II}}{\partial r} & (-h_2 \leq z \leq 0). \end{cases} \tag{19}$$

At $r = r_1$, we have

$$\phi_d^{II} = \phi_d^{III} \quad (-h_2 \leq z \leq -e_1), \tag{20}$$

$$\frac{\partial\phi_d^{II}}{\partial r} = \begin{cases} \frac{\partial\phi_d^{III}}{\partial r} & (-h_2 \leq z \leq -e_1), \\ -\frac{\partial\phi_{inc}}{\partial r} & (-e_1 \leq z \leq 0). \end{cases} \tag{21}$$

4 Solution to the problem

To find the analytical expression for the velocity potential in region I, we apply the channel multipoles method given by Linton and Evans [9] and to find the velocity potential for the regions II and III, we use separation of variables method. Hence, the solution of the boundary-value problem for different regions based on the result of Linton and Evans [9] and Wu et al. [17] are given by

$$\phi_d^I = \sum_{n=0}^{\infty}\sum_{m=0}^{\infty}\sum_{q=0}^{\infty} f_m(z)A_{q,m}\left[U_n(\lambda_m r)\delta_{qn} + E(n,q;m)V_n(\lambda_m r)\right]\cos n\theta, \tag{22}$$

$$\phi_d^{II} = -\phi_{inc} + \sum_{n=0}^{\infty}\sum_{m=0}^{\infty}\left[B_{n,m}S_n(\alpha_m r) + C_{n,m}T_n(\alpha_m r)\right]g_m(z)\cos n\theta, \tag{23}$$

$$\phi_d^{III} = -\phi_{inc} + \sum_{n=0}^{\infty} \left[D_{n,0} J_n(k'r) g_0(z) + \sum_{m=1}^{\infty} D_{n,m} I_n(\alpha_m r) g_m(z) \right] \cos n\theta, \tag{24}$$

where the eigenvalues λ_m and α_m are given by Eqs. (7), (8) and $A_{n,m}$, $B_{n,m}$, $C_{n,m}$ and $D_{n,m}$ are the unknown coefficients which to be determined by applying appropriate matching conditions. The radial functions $U_n(\lambda_m r)$, $V_n(\lambda_m r)$, $S_n(.)$ and $T_n(.)$ are given by

$$a_{2n}(z) = \begin{cases} \cos(2n \sin^{-1} z), & z \le 1 \\ (-1)^n \cosh(2n \cosh^{-1} z), & z > 1, \end{cases} \tag{32}$$

$$a_{2n+1}(z) = \begin{cases} \cos(2n+1) \sin^{-1} z, & z \le 1 \\ i(-1)^n \sinh[(2n+1) \cosh^{-1} z], & z > 1, \end{cases} \tag{33}$$

$$b_{2n+1}(z) = \begin{cases} \sin[(2n+1) \sin^{-1} z], & z \le 1 \\ (-1)^n \cosh[(2n+1) \cosh^{-1} z], & z > 1. \end{cases} \tag{34}$$

Therefore the parameter $E(.,.;.)$ appeared in Eq. (22) is given by

$$E(2p, 2n; m) = \begin{cases} -\dfrac{2i\mu_p}{\pi} \displaystyle\int_0^{\infty} \frac{e^{-k\zeta d} a_{2p}(z) a_{2p}(z)}{\zeta \sinh k\zeta d} dz + \frac{\mu_p}{kd} \sum_{j=0}^{I} \mu_j z_j^{-1} a_{2p}(z_j) a_{2n}(z_j), & m = 0 \\ \mu_p \displaystyle\int_1^{\infty} \frac{e^{-\lambda_m dz} a_{2p}(z) a_{2n}(z)}{\zeta \sinh \lambda_m dz} dz, & m \ge 1 \end{cases} \tag{35}$$

$$E(2p+1, 2n+1; m) = \begin{cases} -\dfrac{4i}{\pi} \displaystyle\int_0^{\infty} \frac{e^{-k\zeta d} b_{2p+1}(z) b_{2n+1}(z)}{\zeta \sinh k\zeta d} dz + \frac{2}{kd} \sum_{j=0}^{I} \mu_j z_j^{-1} b_{2p+1}(z_j) b_{2n+1}(z_j), & m = 0 \\ 2 \displaystyle\int_1^{\infty} \frac{e^{-\lambda_m dz} a_{2p+1}(z) a_{2n+1}(z)}{\zeta \sinh \lambda_m dz} dz, & m \ge 1 \end{cases} \tag{36}$$

$$U_n(\lambda_m r) = H_n^{(1)}(kr), \quad V_n(\lambda_m r)(r) = J_n(kr) \text{ for } m = 0, \tag{25}$$

$$U_n(\lambda_m r) = K_n(\lambda_m r), \quad V_n(\lambda_m r) = I_n(\lambda_m r) \text{ for } m = 1, 2, 3, \ldots, \tag{26}$$

$$S_n(\alpha_m r) = H_n^{(1)}(k'r), \text{ for } m = 0, \tag{27}$$

$$S_n(\alpha_m r) = K_n(\alpha_m r), \text{ for } m = 1, 2, \ldots, \tag{28}$$

$$T_n(\alpha_m r) = H_n^{(2)}(k'r), \text{ for } m = 0, \tag{29}$$

$$T_n(\alpha_m r) = I_n(\alpha_m r), \text{ for } m = 1, 2, \ldots, \tag{30}$$

where $H_n^{(1)}(.)$and $H_n^{(2)}(.)$ are the Hankel functions of first kind and second kind of order n, respectively and the modified Bessel functions of first and second kind of order n are $I_n(.)$ and $K_n(.)$, respectively. Since based on the result of Linton and Evans [9] to construct the channel multipoles for the region I, we have the following functions

$$\zeta(z) = \begin{cases} -i(1-z)^{1/2}, & z \le 1 \\ (z^2-1)^{1/2}, & z > 1, \end{cases} \tag{31}$$

and

$$E(2p, 2n+1; m) = E(2p+1, 2n; m) = 0 \text{ for all } m$$

where the integral for $m = 0$ is taken to be a principal value of integral for all the singularities which satisfies the Helmholtz equation (9) and also integrand considered as a function of complex variable z, has simple poles at $k\zeta d = \pm j\pi i$, $j = 0, 1, 2, \ldots$, i.e. at $z = \pm z_j$ we have

$$z_j = (1 - (j\pi/kd)^2)^{1/2}, \ j = 0, 1, 2, \ldots, I$$

$$z_j = i((j\pi/kd)^2 - 1)^{1/2}, \ j \ge I + 1$$

where $I\pi < kd < (I+1)\pi$.

5 Wave force

The dynamic fluid pressure in terms of velocity potential can be derived from Bernoulli's equation of continuity which is given by

$$P(r, \theta, z, t) = -\rho \frac{\partial \Phi(r, \theta, z, t)}{\partial t}, \tag{37}$$

where ρ is the uniform fluid density. Since wave exciting forces are commonly corresponding to the consolidated activity of incident potential ϕ_{inc} and diffraction's potential ϕ_d. Suppose F_i and F_d are the horizontal force due to the incoming and diffraction potentials, respectively. Hence the total force denoted by F_s and given by

$$F_s = F_i + F_d. \tag{38}$$

Now the horizontal force component F_{i1} corresponding to incident potential and F_{d2} due to diffracted potential acting on the upper cylinder along the x-direction are obtained as

$$F_{i1} = i\rho\omega \int_0^{2\pi} \int_{-e_1}^{0} \phi_{inc}(r_1, \theta, z) r_1 \cos\theta d\theta dz, \tag{39}$$

$$\text{or } F_{i1} = -\frac{2\pi i\rho g r_1 J_1(kr_1)}{\cosh(kH)} \frac{\sinh(kH) - \sinh[k(H-e_1)]}{k} \tag{40}$$

and

$$F_{d2} = i\rho\omega \int_0^{2\pi} \int_{-e_1}^{0} \phi_d^{II}(r_1, \theta, z) r_1 \cos\theta d\theta dz, \tag{41}$$

$$\begin{aligned} \text{or } F_{d2} &= \frac{2\pi i\rho g r_1 J_1(kr_1)}{\cosh(kH)} \frac{\sinh(kH) - \sinh[k(H-e_1)]}{k} \\ &\quad - i\rho\pi\omega r_1 \sum_{m=0}^{\infty} N_m^{-1/2} \times \\ &\left[B_{1,m} S_1(\alpha_m r_1) + C_{1,m} T_1(\alpha_m r_1)\right] \frac{\sin(\alpha_m h_2) - \sin(\alpha_m e_2)}{\alpha_m}, \end{aligned} \tag{42}$$

where $e_2 = h_2 - e_1$ i.e. gap between the cylinders as shown in Fig. 1. Now by using Eqs. (38), (40) and (42), we can derived the total horizontal force F_{s1} exerted by the upper cylinder and it can be given by

$$\begin{aligned} F_{s1} &= -i\rho\pi\omega r_1 \sum_{m=0}^{\infty} N_m^{-1/2} \left[B_{1,m} S_1(\alpha_m r_1) \right. \\ &\quad \left. + C_{1,m} T_1(\alpha_m r_1)\right] \frac{\sin(\alpha_m h_2) - \sin(\alpha_m e_2)}{\alpha_m}. \end{aligned} \tag{43}$$

The non-dimensional horizontal force exerted by the floating cylinder can be obtained divide by $u_0 = \rho g \pi {r_1}^2$ to F_{s1} and it is given by

$$\begin{aligned} F_{s1}/u_0 &= \frac{-i\omega}{g r_1} \sum_{m=0}^{\infty} N_m^{-1/2} \left[B_{1,m} S_1(\alpha_m r_1) \right. \\ &\quad \left. + C_{1,m} T_1(\alpha_m r_1)\right] \frac{\sin(\alpha_m h_2) - \sin(\alpha_m e_2)}{\alpha_m}. \end{aligned} \tag{44}$$

The exciting force F_{d3} acting on the inner wall of the upper cylinder due to the diffracted potential ϕ_d^{III} in region *III* can be expressed as

$$\begin{aligned} F_{d3} &= \frac{2\pi i\rho g r_1 J_1(kr_1)}{\cosh(kH)} \frac{\sinh(kH) - \sinh[k(H-e_1)]}{k} \\ &\quad - i\rho\pi\omega r_1 \sum_{m=0}^{\infty} N_m^{-1/2} \\ &\quad \times D_{1,m} I_1(\alpha_m r_1) \frac{\sin(\alpha_m h_2) - \sin(\alpha_m e_2)}{\alpha_m}. \end{aligned} \tag{45}$$

Similarly, we derived the expression for the total horizontal force F_{s2} exerted by the bottom-mounted cylinder due to diffracted velocity potential ϕ_d^I and incident velocity potential ϕ_{inc} in region *I* and it can written as

$$\begin{aligned} F_{s2} &= -i\rho\pi\omega r_2 \sum_{m=0}^{\infty} \sum_{q=0}^{\infty} A_{q,m} M_m^{-1/2} \left[U_{1,m}(\lambda_m r_2)\delta_{q,1} \right. \\ &\quad \left. + E(1,q;m) V_{1,m}(\lambda_m r_2)\right] \times \\ &\quad \frac{\sin\lambda_m(H-h_2)}{\lambda_m}. \end{aligned} \tag{46}$$

In order to make it non-dimensionalized, we divide by $u_1 = \rho g \pi r_2^2$ to F_{s2}, which gives

$$\begin{aligned} F_{s2}/u_1 &= \frac{-i\omega}{g r_2} \sum_{m=0}^{\infty} \sum_{q=0}^{\infty} A_{q,m} M_m^{-1/2} \left[U_{1,m}(\lambda_m r_2)\delta_{q,1} \right. \\ &\quad \left. + E(1,q;m) V_{1,m}(\lambda_m r_2)\right] \\ &\quad \times \frac{\sin\lambda_m(H-h_2)}{\lambda_m}. \end{aligned} \tag{47}$$

6 Numerical results and conclusion

From the above discussions, we have seen that to get horizontal exciting forces, we have to evaluate the associated unknown coefficients appearing in the expressions of potentials given by the Eq. (22–24) with the help of matching conditions (18–21). As every expression of potential is found to be a series with infinite terms, therefore, calculate the corresponding values, we must be truncated appropriately after some terms. For our convenience, let us truncate all the infinite series into a limited number of terms by assuming $M = 30$. Proceeding in this way, we arrived at a system of simultaneous linear equations with aforesaid unknown coefficients. Then the solutions of these unknown coefficients corresponding to above system of linear equations are obtained by using MATLAB programming. Once found the unknown coefficients, then the velocity potentials allow to find the exciting forces exerted

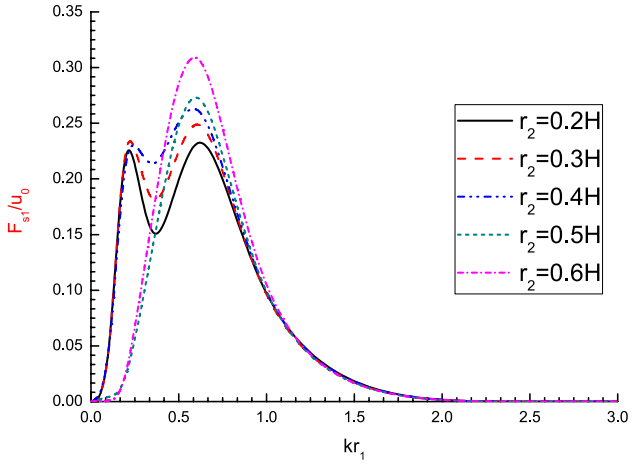

Fig. 2 Variation of dimensionless horizontal exciting force F_{s1}/u_0 versus dimensionless wave number kr_1 for different radii of the lower cylinder r_2 with $e_1 = 0.1H, r_1 = 0.2H, d = 0.8H$

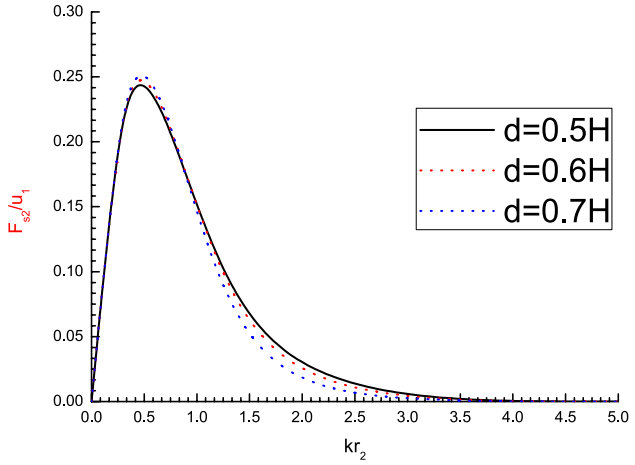

Fig. 4 Variation of dimensionless horizontal exciting force F_{s2}/u_1 versus dimensionless wave number kr_2 for different width of the channel walls d with $r_1 = 0.2H, r_2 = 0.4H, e_1 = 0.1H$

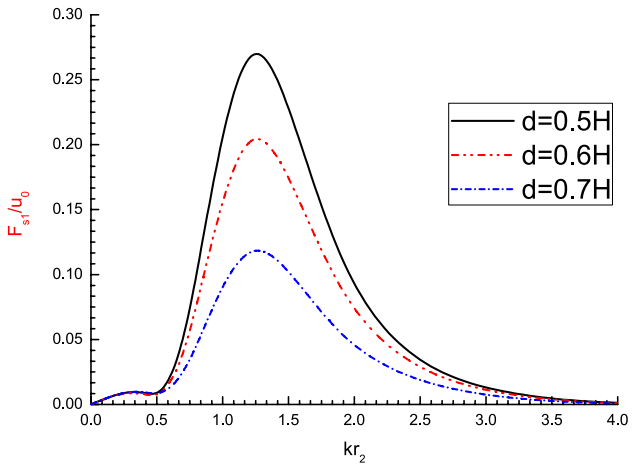

Fig. 3 Variation of dimensionless horizontal exciting force F_{s1}/u_0 versus dimensionless wave number kr_2 for different width of the channel walls d with $r_1 = 0.2H, r_2 = 0.4H, e_1 = 0.1H$

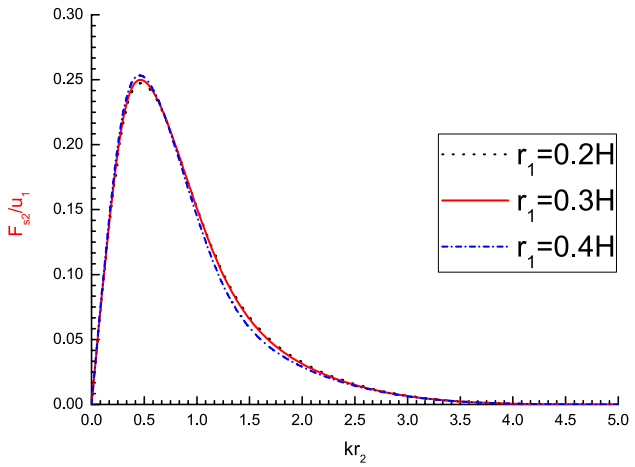

Fig. 5 Variation of dimensionless horizontal exciting force F_{s2}/u_1 versus dimensionless wave number kr_2 for different radius of the hollow cylinder r_1 with $e_1 = 0.1H, r_2 = 0.4H, d = 0.6H$

by the cylinder. We discussed the influence of the various parameters like radius, draft of cylinder (submerged part), the gap between the cylinders and mainly width of the channel walls on the exciting forces. Let us consider the values of the parameters throughout our calculations as $H = 3\,\text{m}, g = 9.807\,\text{m/s}^2$ and $e_2 = 0.25H$. For fixed $r_1 = 0.2H$, we proceed to study the effect on the horizontal exciting force of the floating cylinder due to the radius of the lower cylinder. In Fig. 2, we plot F_{s1}/u_0 against kr_1 taking distinct values of radius to the bottom-mounted cylinder say $r_2 = 0.2H, 0.3H, 0.4H, 0.5H, 0.6H$. From Fig. 2, we saw that no oscillation happens for those value of r_2 when $r_2 > \frac{1}{2}d$. Also we observed oscillation for higher value of r_2, e.g. $r_2 = 0.2H$ and $0.3H$ in which case $r_2 \leq \frac{1}{2}d$. It is likewise seen that the oscillation, at whatever point they happen, just at lower values of k. Again when $r_2 \leq \frac{1}{2}d$, it is seen that peak value of exciting force occurs at more than one points. For all values of r_2, the exciting force attains its most extreme value only at lower range of k. For higher value of k, the force relentlessly lesser achieving right around zero. It is to be noted that when the radius of lower cylinder increases, the force exerted by cylinder is decreases. Next we investigate the effect of width of the channel walls on the exciting forces on the upper and lower cylinders. Here we fixed the parameters r_2, r_1 and e_1 by choosing $r_2 = 0.4H$, $r_1 = 0.2H$ and $e_1 = 0.1H$. In Figs. 3 and 4, we plot F_{s1}/u_0 and F_{s2}/u_1 against kr_2, respectively, for different values of width of channel walls, $d = 0.5H, 0.6H, 0.7H$. From Fig. 3, we

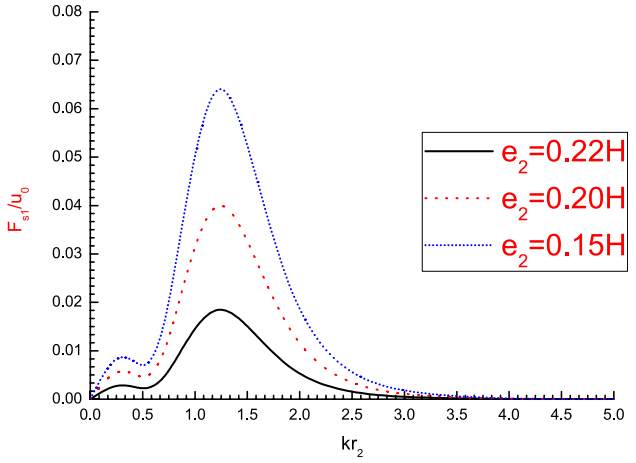

Fig. 6 Variation of dimensionless horizontal exciting force F_{s1}/u_0 versus dimensionless wave number kr_2 for different gap ($e_2 = h_2 - e_1$, for a fixed h_2) between the cylinders with $r_1 = 0.2H$, $r_2 = 0.4H$, $d = 0.6H$

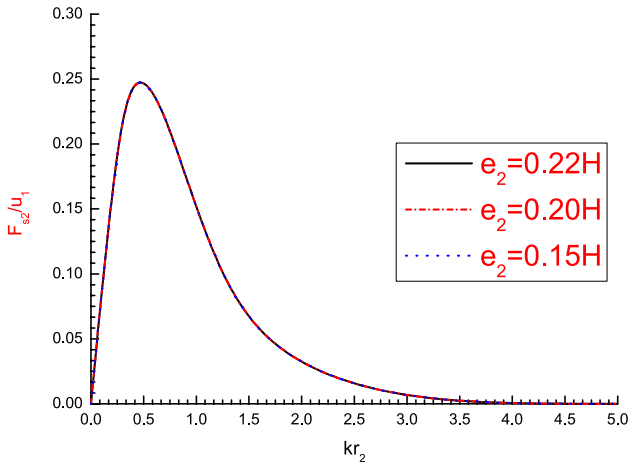

Fig. 7 Variation of dimensionless horizontal exciting force F_{s2}/u_1 versus dimensionless wave number kr_2 for different gap ($e_2 = h_2 - e_1$, for a fixed h_2) between the cylinders with $r_1 = 0.2H$, $r_2 = 0.4H$, $d = 0.6H$

observed that the values of the exciting force increases with width of the channel walls decreases and Fig. 4 show that similar effect on exciting force on the upper cylinder. Remarkably both the exciting forces attains maximum value only for lower value of wave number k and forces are almost vanishing for higher value of k.

Now we determine the variation of exciting forces on the cylinders for different radius of the hollow cylinder. When we compute the exciting forces for different r_1, we fixed the value of r_2, e_1 and d by taking $r_2 = 0.4H$, $e_1 = 0.1H$ and $d = 0.6H$. In Fig. 5, we plot F_{s2}/u_1 against kr_2 for distinct values of radius to the hollow cylinder, $r_1 = 0.2H$, $0.3H$, $0.4H$. Figure 5 shows that the forces

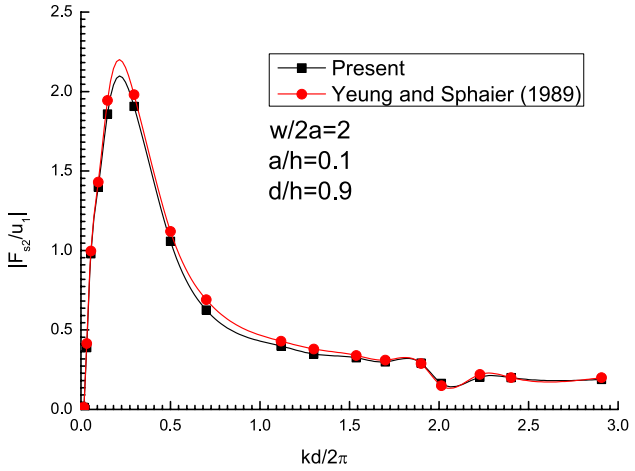

Fig. 8 Comparison of exciting force F_{s2}/u_1 with result of Yeung and Sphaier [19] with $r_2/H = 0.1$, $d/H = 0.2$ and $h_2/H = 0.1$

increases with the decreasing radius r_1. For $r_1 = 0.2H$, the dimensionless force F_{s2}/u_1 attains the maximum values equal to 0.251901. The highest values of the forces occurs only at values of lower range of k.

Again for fixed r_2 by taking $r_2 = 0.4H$, now proceed to investigate how the exciting forces on the upper and lower cylinders are affected by the gap between the cylinders. In Figs. 6 and 7, we plot F_{s1}/u_0 and F_{s2}/u_1 against kr_2, respectively, for different values of e_2, say, $e_2 = 0.22H$, $0.20H$, $0.15H$, i.e. for $e_1 = 0.03H$, $0.05H$, $0.1H$, respectively. Figure 6 clearly shows that as the e_2 decreases, the force increases only at lower values of k, i.e. the larger value of exciting force happen for $e_2 = 0.15H$, i.e. $e_1 = 0.1H$ and Fig. 7 shows that deviation of exciting force is very negligible for different gap between the cylinders.

Now it is reasonable to compare our results with the results of Yeung and Sphaier [19] for the modulus of the non-dimensional horizontal exciting force. All the parameters considered in our problem are reconsidered according to the ones from Yeung and Sphaier's work in order to have the same physical problem. So we consider the value of the draft $e_1 = 0.0001$ in order to have a single structure as in Yeung and Sphaier [19]. The values of the other parameters are considered as: $r_2/H = 0.1$, $d/H = 0.2$ and $h_2/H = 0.1$ and draft of lower cylinder $e_3 = H - h_2$. In the Yeung and Sphaier [19] the parameters a, d, w represent radius, a draft of the cylinder and the width of the channel wall, respectively. The comparison of both the results is shown in Fig. 8 and Fig. 8 shows good agreement between the results of the present work and Yeung and Sphaier [19]. Also Table 1 shows the numerical comparison between the results of present work and Yeung and Sphaier [19]. It shows good numerical comparison between both the results.

Table 1 Comparison of exciting force F_{s2}/u_1 with numerical results of Yeung and Sphaier [19] along with the parameters $r_2/H = 0.1$, $d/H = 0.2$ and $h_2/H = 0.1$

Frequency ($f = \omega/2\pi$)	Yeung and Sphaier [19]	Present
0.15	0.0119	0.01254612510259
0.25	0.4154	0.38952874560142
0.37	0.9968	0.9789742150271
0.5	1.4312	1.3989512540521
0.62	1.9445	1.85915744551101
0.8	1.9801	1.90627096010328
1.0	1.1223	1.05816611655631
1.28	0.6912	0.6251542364021
1.5	0.4321	0.39853546452436
1.7	0.3801	0.34814785208
2.0	0.3412	0.32513654785256
2.4	0.3132	0.29881546010191
2.5	0.3501	0.29124564556092
2.6	0.2892	0.29125416527361
2.65	0.1512	0.16335512642084
2.75	0.2212	0.20345512642674
2.78	0.2012	0.19984657552216

Acknowledgements The authors wishes to thank North Eastren Regional Institute of Science and Technology, Itanagar for providing necessary facilities. This work was supported by the Department of Science and Technology, SERB, [Grant Number: SERB (YSS/14/000884)], Govt. of India. The authors are very much grateful to the esteemed reviewer whose comments and suggestions empowered the revised version of the manuscript become a much better form in terms of presentation.

Compliance with ethical standards

Conflict of interest On behalf of all authors, the corresponding author states that there is no conflict of interest.

References

1. Bharatkumar BH, Mahadevan R, Pranesh MR (1991) Flume confinement effect on diffracted wave field around vertical cylinders. Ocean Eng 18:521–533
2. Bhatta DD, Rahman M (2003) On scatering and radiation problem for a cylinder in water of finite depth. Int J Eng Sci 41(9):931–967
3. Bhattacharjee J, Soares CG (2010) Wave interaction with a floating rectangular box near a vertical wall with step type bottom topography. J Hydrodyn 22(5):91–96
4. Buffer BP, Thomas GP (1993) The diffraction of water waves by an array of circular cylinders in a channel. Ocean Eng 20:296–311
5. Hassan M, Bora SN (2012) Exciting forces for a pair of coaxial hollow cylinder and bottom-mounted cylinder in water of finite depth. Ocean Eng 50:38–43
6. Hassan M, Bora SN (2014) Hydrodynamic coefficients for a radiating hollow cylinder placed above a coaxial cylinder at finite ocean depth. J Mar Sci Technol 19:450–461
7. Kashiwagi M (1991) Radiation and diffraction forces acting on an offshore-structure model in a towing tank. Int J Offshore Polar Eng 1:101–107
8. Linton CM (1993) On the free-surface Green's function for channel problems. Appl Ocean Res 15:263–267
9. Linton CM, Evans DV (1992) The radiation and scattering of surface waves by a vertical circular cylinder in a channel. Phil Trans R Soc Lond A 338:325–357
10. Martins-rivas H, Mei CC (2009a) Wave power extraction from an oscillating water column along a staright coast. Ocean Eng 36(6–7):426–433
11. Martins-rivas H, Mei CC (2009b) Wave power extraction from an oscillating water column at the tip of the brealwater. J Fluid Mech 626:395–414
12. Mclver P, Bennett GS (1993) Scattering of water waves by axisymmetric bodies in a channel. J Eng Math 27:1–29
13. MacCamy RC, Fuchs, RA (1954) Wave forces on piles: a diffraction theory. Technical memo, no. 69. US Army Beach Erosion Board, 17
14. Neelamani S, Bharatkumar BH, Mahadevan R, Sundar V (1993) Flume confinement effect on wave-induced dynamic pressures on twin-tandem cylinders. Ocean Eng 20:313–337
15. Thomas GP (1991) The diffraction of water waves by a circular cylinder in a channel. Ocean Eng 18:17–44
16. Thorne RC (1953) Multipole expansions in the theory of surface waves. Proc Camb Phil Soc 49:707–716
17. Wu BJ, Zheng YH, You YG, Sun XY, Chen Y (2004) On scattering and radiation problem for a cylinder over a cylindrical barrier in water of finite depth. Eng Sci 6(2):48–55 **(in Chinese)**
18. Wu BJ, Zheng YH, You YG (2006) Response amplitude and hydrodynamic force for a buoy over a convex. J Waterw Port Coast Ocean Eng 132(2):97–105
19. Yeung RW, Sphaier SH (1989) Wave-interference effects on a truncated cylinder in a channel. J Eng Math 23:95–117
20. Zhu SP, Mitchell L (2009) Diffraction of ocean waves around a hollow cylindrical shell structure. Wave Motion 46:78–88
21. Zheng S, Zhang Y, Iglesias G (2019) Coast/breakwater-integrated OWC: a theretical model. Mar Struct 66:121–135